NeuroImage xxx (2018) xxx-xxx

Contents lists available at ScienceDirect

NeuroImage

journal homepage: www.elsevier.com

Implicit visual cues tune oscillatory motor activity during decision-making

Andrea Alamia[a, b], Alexandre Zénon[a, 1], Rufin VanRullen[b], Julie Duque[a], Gerard Derosiere[a, *]

[a] Institute of Neuroscience, Université catholique de Louvain, Brussels, Belgium
[b] Centre de Recherche Cerveau et Cognition, Université Paul Sabatier, Toulouse, France

ARTICLE INFO

Keywords:
Motor decision
EEG
Oscillations
Unconscious
Action selection

ABSTRACT

Motor decisions entails a buildup of choice-selective activity in the motor cortex. The rate of this buildup crucially depends on the amount of evidence favoring the selection of each action choice in the visual environment. Though numerous studies have characterized how sensory evidence drives motor activity when processed consciously, very little is known about the neural mechanisms that underlie the integration of implicit sources of information.

Here, we used electroencephalography to investigate the impact of implicit visual cues on response-locked potentials and oscillatory activity in the motor cortex during decision-making. Subjects were required to select between left and right index finger responses according to the motion direction of a cloud of dots presented in one of three possible colors. Unbeknown to the participants, the color cue could bring evidence either *in favor of* or *against* the selection of the correct response.

Implicit color cues tuned choice-selective oscillatory activity in the low beta range (16–25 Hz), boosting the buildup of contralateral activity when evidence favored the selection of the correct action, while weakening it when evidence biased against the correct response. This modulation of oscillatory activity influenced the speed at which the correct action was eventually chosen. Implicit cues also altered oscillatory activity in a non-selective way in the low frequency oscillation (1–7 Hz) and high beta ranges (25–35 Hz), impacting both contralateral and ipsilateral activity. The current findings yield a critical extension of prior observations by indicating that the integration of both explicit and implicit sources of evidence tunes oscillatory motor activity during decision-making.

1. Introduction

A recent theoretical framework upholds that motor decisions arises from a competition between the representations of the different possibilities of action provided by the environment (Cisek and Pastor-Bernier, 2014; Pezzulo and Cisek, 2016; Derosiere et al., 2017a, 2017b). In this view, separate action opportunities evoke increases in activity in distinct neural populations within the motor system (Thura and Cisek, 2014, 2017), which compete with one another through mutual inhibition (Shen et al., 2010). An action is eventually selected and executed when activity in the related population reaches a critical decision threshold (Lo and Wang, 2006; Von Reyn et al., 2014; Jha et al., 2016).

Consistent with this idea, several lines of evidence indicate that the motor cortex displays a buildup of choice-selective activity during decision-making. Indeed, electrophysiological studies have revealed that the motor area contralateral to a chosen effector exhibits a progressive increase in the amplitude of evoked potentials, a synchronization of low frequency oscillations (LFO, [1–7 Hz]), and a desynchronization of beta frequency oscillations (BFO, [15–35 Hz], often referred to as beta-band event-related desynchrony [β-ERD]) as action execution draws nearer (Kubanek et al., 2013; Nguyen et al., 2014; Noorbaloochi et al., 2015; Waldert et al., 2015; Burle et al., 2016; Herding et al., 2016; Meijer et al., 2016; Murphy et al., 2016; Popovych et al., 2016; Derosiere et al., 2018). Interestingly, the rate of this buildup was shown to depend on the amount of evidence indicating the appropriate action to select in the visual environment: when evidence for an action is strong, activity in the contralateral motor cortex grows faster than when it is weak, increasing its likelihood to reach the decision threshold (Tosoni et al., 2008, 2014; Donner et al., 2009; Gould et al., 2012; Wyart et al., 2012; Grent-'t-Jong et al., 2013). Such a modulation of

* Corresponding author. CoActions Lab, Institute of Neuroscience, Université catholique Louvain, Av. Mounier, 53 - Bte B1.53.04, 1200, Bruxelles, Belgium.
Email address: gerard.derosiere@uclouvain.be (G. Derosiere)
[1] Present address: INCIA, Unité Mixte de Recherche, Centre National de la Recherche Scientifique, Bordeaux, France.

https://doi.org/10.1016/j.neuroimage.2018.11.027
Received 7 September 2018; Received in revised form 5 November 2018; Accepted 16 November 2018
Available online xxx
1053-8119/

motor activity helps understand why decision speed and accuracy are both boosted when evidence clearly favors an action (Loughnane et al., 2016; Paz et al., 2016; Herz et al., 2017).

Importantly, the abundance of stimuli in the visual environment impedes the nervous system to process all of them with the same degree of conscious awareness. Hence, part of the visual information used to guide motor decisions remains implicit (Mayr, 2004; Sumner et al., 2007; van Gaal et al., 2010; Alamia et al., 2016; Derosiere et al., 2017a, 2017b). Strikingly, though numerous studies have characterized how sensory evidence drives choice-selective motor activity when provided through explicit cues (Tosoni et al., 2008; Donner et al., 2009; Gould et al., 2012; Wyart et al., 2012), very little is known about the neural mechanisms that underlie the integration of implicit sources of information. In fact, the findings of a former electroencephalography (EEG) study indicate that subliminal priming stimuli may bias action choices by tuning potential amplitudes in the motor cortex (Dehaene et al., 1998). Yet, whether and how implicit sensory signals influence oscillatory motor activity remain open questions.

In the present study, we used EEG to investigate the impact of implicit visual cues on response-locked potentials and oscillatory activity in the motor cortex during decision-making. Subjects performed a random dot motion (RDM) task which required them to select between left and right index finger responses according to the dominant motion direction of a cloud of dots presented in one of three possible colors. Unbeknown to the participants, the color cue could bring evidence in favor of one of the two motor responses. In fact, two of the three colors were frequently associated with a given motion direction (*i.e.*, 80% of the time), hence providing subjects with additional evidence regarding the correct response (Alamia et al., 2016). Besides, when presented with the opposite motion direction, these two colors yielded evidence against the selection of the correct response (*i.e.*, they prompted subjects to select the incorrect response; 20% of occurrence). The third color appeared in equal proportions for both motion directions and was uninformative regarding the correct response.

2. Materials and methods

2.1. Participants

18 healthy naive subjects participated in this study (13 women, 24.3 ± 1.8 years old). All subjects were right-handed according to the Edinburgh Questionnaire and had normal or corrected-to-normal vision. None of the participants had any neurological disorder, history of psychiatric illness, drug or alcohol abuse, or were under any drug treatment that could influence performance. Participants were financially compensated for their participation. The protocol, in agreement with the Declaration of Helsinki, was approved by the institutional review board of the Université Catholique de Louvain, Brussels, Belgium, and required written informed consent signed by each participant.

2.2. Experimental design

Subjects sat on a comfortable chair in front of a 21-inches cathode ray tube computer screen, with their head supported by a chinrest at 60 cm from the monitor. The refresh rate was set at 100 Hz. The left and right forearms were placed on the surface of the table with each hand holding a computer mouse. The left and the right index fingers were positioned over the right and left buttons of the left and right mice, respectively. Participants wore a 32 Ag/AgCl electrode EEG cap placed according to the international 10/20 system during the experiment (Waveguard 32 cap, Cephalon A/S, Denmark). EEG signals were amplified and digitized using a sampling rate of 1000 Hz (32-channel high-speed amplifier, Advanced Neuro Technology, The Netherlands). Electrode impedances were kept below 10 kΩ. An average reference was exploited for all recordings.

2.3. Task

We used the RDM task (Murphy et al., 2016). The task was implemented in Matlab 7.5 (The Mathworks, Natick, Massachusetts, USA) using the Psychophysics toolbox, version 3.0.9 (Brainard, 1997). Each trial started with the presentation of a warning signal, a white fixation cross (+), displayed at the centre of the gray screen for 600 ms. This signal indicated the beginning of the trial. Then, a cloud of moving dots appeared for 300 ms before being replaced by a gray screen. Subjects were required to select between left or right index finger responses as accurately as possible according to the dominant motion direction of the dots (*i.e.*, left and right directions, respectively). In the absence of response, the gray screen disappeared after a delay of 1000 ms from the onset of the cloud, and the response was considered as incorrect (less than 1% of the trials). An auditory feedback was provided at the end of each trial; high- and low-pitch sounds indicated correct and incorrect responses, respectively. The time course of a typical trial is depicted in Fig. 1A.

Importantly, in each trial, the cloud of dots could be colored in either red, green or blue. Unbeknown to the subjects, two of the three colors (*e.g.*, red and green) occurred in different proportions in trials involving left and right motion directions, while the third color (*e.g.*, blue) appeared in equal proportions for both directions (see Fig. 1B; the color-to-motion assignment was counterbalanced across subjects). As such, one color (*e.g.*, red) occurred 80% of the time when the motion direction was left, and only 20% of the time when it was right. Conversely, another color (*e.g.*, green) occurred 80% of the time when the motion direction was right, and only 20% of the time when it was left. Hence, some trials involved a highly frequent color-motion association (*i.e.*, "red-left" and "green-right" in the above example), while other trials entailed a very unlikely one (*i.e.*, "red-right" and "green-left" in the example).

The color of the dots was exploited as an implicit cue (I-Cue) to provide subjects with evidence either *for* or *against* the correct motor response, depending on whether the trial involved a frequent or an unlikely color-motion association (see Fig. 1B; Alamia et al., 2016; Derosiere et al., 2017a, 2017b). In the former trial type (*i.e.*, involving a frequent association), the color yielded evidence *for* the selection of the correct response, hence helping subjects to select this response; we call these trials "I-Cue$_{For}$ trials". Contrariwise, in the latter trial type (*i.e.*, unlikely association), the color presented to the subject corresponded to the one mostly associated with the opposite motion direction. Hence, it yielded evidence *against* the selection of the correct response (*i.e.*, it brought evidence for the selection of the incorrect response); we call these trials "I-Cue$_{Against}$ trials". Finally, the color assigned in equal proportion to both motion directions was uninformative regarding the correct response; we call these trials "I-Cue$_{Neutral}$ trials". I-Cue$_{Neutral}$ trials served as the control condition. Note that to ensure that subjects paid attention to the color of the dots throughout the experiment, we asked them to report it in 10% of the trials. During these trials, three circles (*i.e.*, one of each color) were simultaneously displayed to the participants following feedback presentation; participants were asked to report the color they saw in the last cloud of dots (*i.e.*, in the last trial realized) by clicking on the corresponding circle with the right mouse. There was no time-limit and participants were provided with high- (low-) pitch auditory feedback in case of correct (incorrect) response. These trials occurred pseudo-randomly in each block.

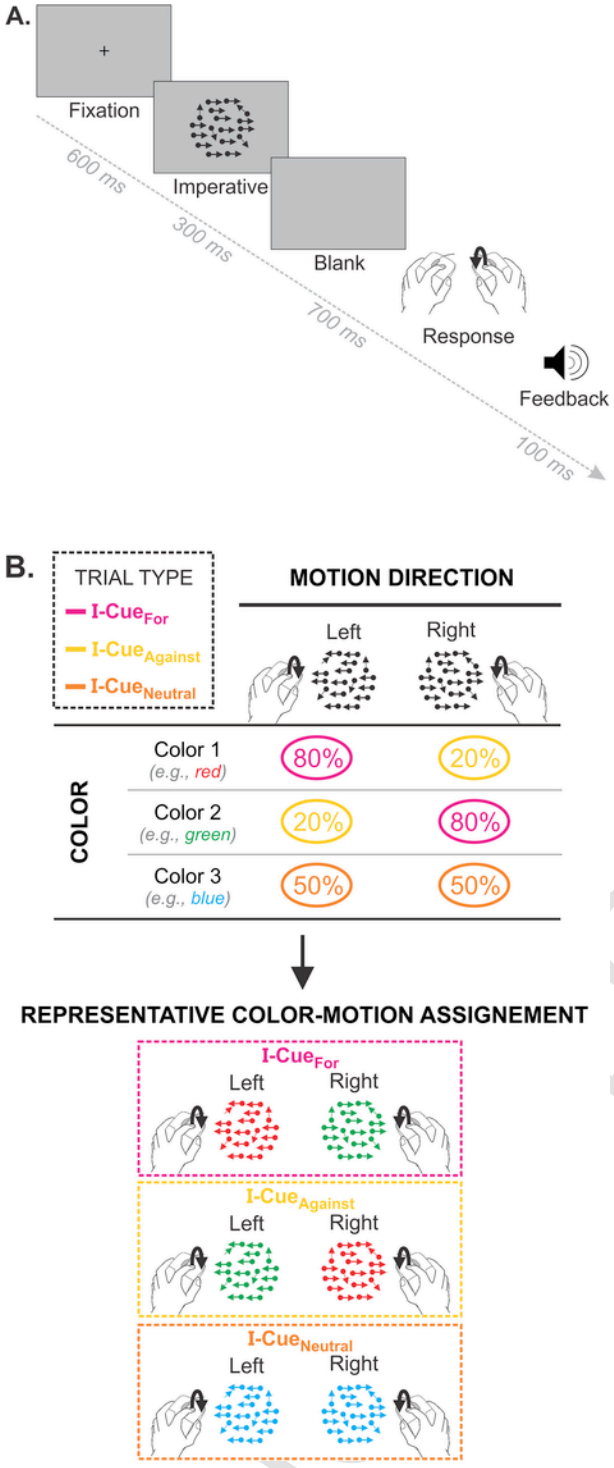

Fig. 1. Task. A. In this typical trial, the dominant motion direction is right, as represented by the small black arrows in the cloud. For representative purposes, the number of dots was reduced. **B.** I-Cue$_{For}$ trials (pink) involved a frequent color-motion association: hence, the color cue implicitly provided the subjects with additional evidence for the selection of the correct motor response. Conversely, I-Cue$_{Against}$ trials (yellow) involved an unlikely color-motion association: here, the color cue corresponded to the one frequently associated with the opposite motion direction, hence providing participants with evidence against the selection of the correct response (*i.e.*, by prompting subjects to select the incorrect one). Finally, in I-Cue$_{Neutral}$ trials (orange), the color was assigned in equal proportion to both motion directions and was uninformative regarding the appropriate action to select. (For interpretation of the references to color in this figure legend, the reader is referred to the Web version of this article.)

2.4. Experimental protocol

Each experiment started with a training stage composed of 8 blocks of 60 trials, with each block lasting 3 min. During this training, participants performed the RDM task without color manipulation (*i.e.*, the cloud of dots was black on gray background), and the motion coherence (*i.e.*, the percentage of dots moving coherently in the same direction) was adapted after each block. The coherence was set at 100% in the first block to enable the subjects to familiarize with the task, and was then decreased to 90% in the second block. In the following blocks, the coherence was either *(1)* increased by 5% if the proportion of correct choices (*i.e.*, accuracy) was lower than 0.6, *(2)* kept constant if accuracy was between 0.6 and 0.8, or *(3)* decreased by 10% if accuracy was higher than 0.8. The goal of this procedure was to ensure that all participants started the color-based version of the RDM task (see *Task* section) with an average accuracy of 0.7.

Once the training stage was completed, the EEG cap was set and participants performed the color-based RDM task; 8 blocks of 60 trials were realized, during which motion coherence was kept constant. Participants were allowed to have short pauses between each block. The whole experiment lasted approximately 90 min.

2.5. Explicit tests and questionnaire

Participants were never told about the association between the colors and the motion directions. However, in order to control for the implicit nature of the association empirically, each subject underwent a questionnaire immediately after having completed the last block of trials (see Alamia et al., 2016; Derosiere et al., 2017a, 2017b, for a similar procedure). Subjects were asked the three following questions (originally in French): 1. "*Did you perceive any difference in the cloud of dots between the rightward and leftward motion directions?*"; 2. "*Did you feel any difference in the perception of the motion direction when presented with the red, the green or the blue color?*"; 3. "*Did you notice any association between the motion directions or the finger responses and the color of the dots?*". They were required to answer in a written form. None of the participants answered positively to the third question.

Importantly, the results of our previous study (Alamia et al., 2016) showed that participants who fail to report the association in such questionnaires, also fail to report the association in more sensitive tests, such as in generative and familiarity tests (Newell and Shanks, 2014). The results obtained in these tests in Alamia et al. (2016) are presented in Fig. 2 (n = 18). Three tests were performed. First, a generative motion test was realized (Fig. 2A): participants were presented with a static but colored cloud of dots and were asked to associate a motion direction with the color. Second, a generative color test was performed (Fig. 2B): here, participants were presented with a patch of black dots moving either to the left or to the right direction and were asked to associate one of the three colors with the motion direction. Finally, a familiarity test was realized (Fig. 2C): participants were asked to rate, from 1 to 10, how familiar they found different moving and colored clouds of dots, representing the color-motion associations they encountered in the three trial types of the experiment (*i.e.*, I-Cue$_{For}$, I-Cue$_{Against}$and I-Cue$_{Neutral}$). Each generative test comprised 30 trials and the familiarity test comprised 42 trials.

A Bayes Factor (BF) analysis of the data obtained in the generative motion test (Fig. 2A) revealed that the probability of choosing a given motion direction over another did not statistically depend on the color presented (*i.e.*, left motion-associated color, right motion-associated color or neutral color; BF value = 90.01, p = .02). This indicates that subjects selected to a comparable extent the left and right motion directions, independently of the color they were presented with, thus revealing a lack of awareness of the color-motion associations which

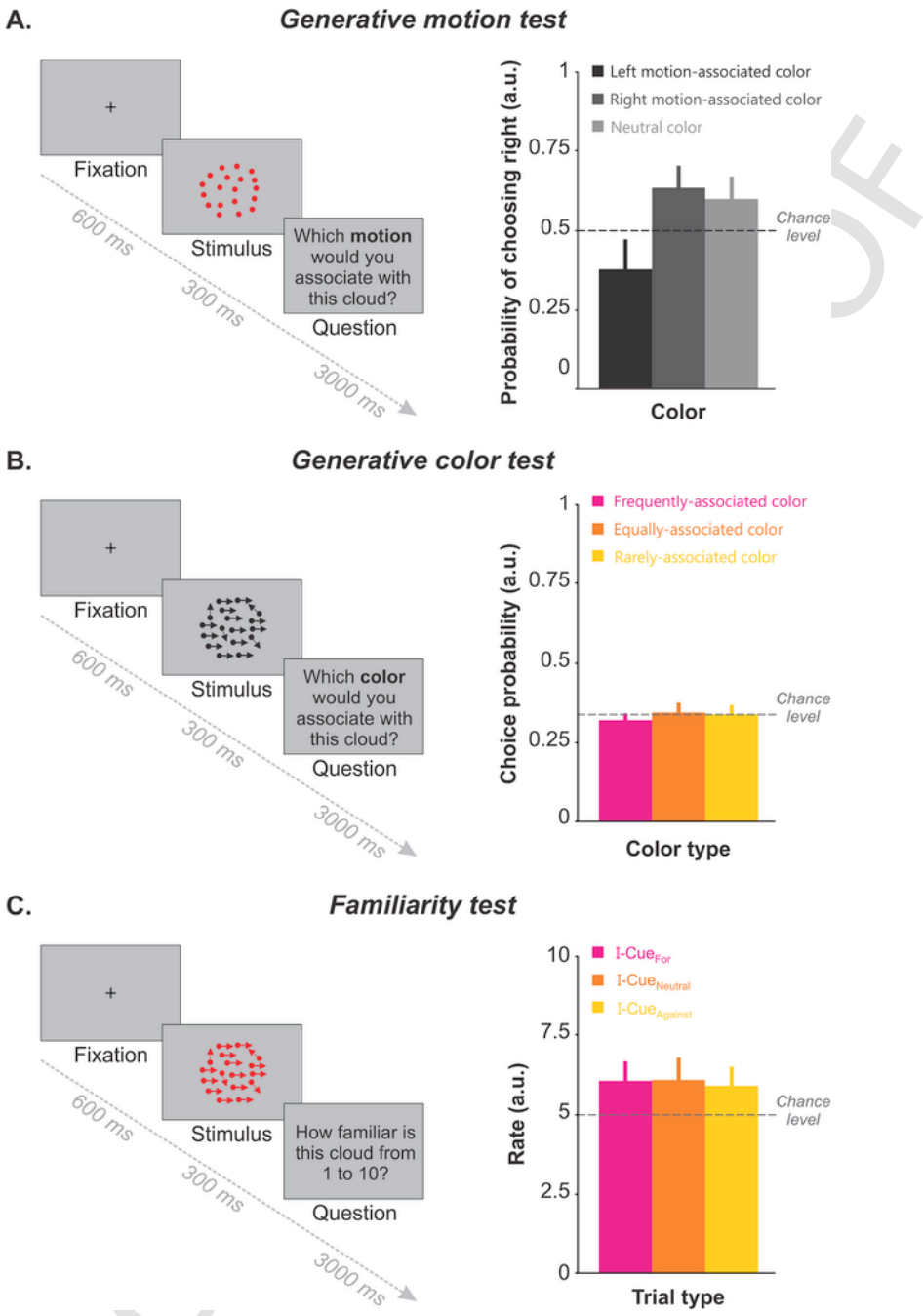

Fig. 2. Explicit tests (performed on a sample in 18 subjects; data from Alamia et al., 2016). **A.** *Left:* Time course of a trial in the generative motion test. *Right:* Results obtained in the generative motion test. The probability of choosing the right motion direction is displayed (y-axis) for each color presented (x-axis; *i.e.*, left motion-associated color [black], right motion-associated color [dark gray] and neutral color [light gray]). The graph suggests that the probability of choosing a given motion direction did not to depend on the color presented. **B.** *Left:* Time course of a trial in the generative color test. *Right:* Results obtained in the generative color test. Values on the y-axis represent the probability of choosing one of the three color types displayed along the x-axis (*i.e.*, color frequently associated [pink], rarely associated [orange] and equally associated [yellow] with the displayed motion direction). The graph shows that each color type was selected to the same extent by the subjects. **C.** *Left:* Time course of a trial in the familiarity test. *Right:* Results obtained in the familiarity test. The familiarity ratings are represented (y-axis) for each of the three trial types (I-Cue$_{For}$, I-Cue$_{Against}$ and I-Cue$_{Neutral}$ trials). The graph indicates that subjects did not report finding a given trial type more familiar than another, despite the higher (lower) rate of occurrence of I-Cue$_{For}$ trials (I-Cue$_{Against}$ trials) compared to I-Cue$_{Neutral}$ ones in the RDM task. (For interpretation of the references to color in this figure legend, the reader is referred to the Web version of this article.)

were embedded in the RDM task. Similarly, the BF analysis performed on the data obtained in the generative color test (Fig. 2B) showed that the probability of choosing a given color over another did not statistically depend on the motion direction presented (*i.e.*, left or right motion direction; BF value = 33.11 p = .03). This reveals that subjects selected to a comparable extent each color, independently of the motion direction they were presented with, confirming that participants were unable to explicitly report the color-motion associations. Finally, the BF analysis performed on the data obtained in the familiarity test (Fig. 2C) revealed that the rating scores – representing how much subjects felt familiar with each cloud of dots – did not statistically depend on the trial type they were presented with (BF value = 38.11, p = .03). This last result shows that subjects were unaware that specific color-motion associations were more frequent (*e.g.*, I-Cue$_{For}$ trials) than others (*e.g.*, I-Cue$_{Against}$).

Altogether, the results obtained in the questionnaire, in the generative tests and in the familiarity test of our previous study (Alamia et al., 2016) coherently indicate that subjects were unaware of the color-motion associations at the end of the experiment. Hence, it is reasonable to assert that the informative value of the color cue remained implicit in the present study (Destrebecqz and Peigneux, 2005; Gaillard et al., 2014; Derosiere et al., 2017a, 2017b).

2.6. Data analyses

2.6.1. Behavioral data

Finger responses were classified according to the trial type in which they were provided (*i.e.*, I-Cue$_{For}$, I-Cue$_{Neutral}$ and I-Cue$_{Against}$ trials; left and right motion directions pooled together). For each trial type, we calculated the proportion of correct responses (accuracy) and their reaction times (RTs).

2.6.2. EEG data

All EEG data were processed on Matlab (The Mathworks Inc. Natick, Massachusetts, USA) using Letswave 6 (Mouraux and Iannetti, 2008). The EEG signals were filtered using a 0.01–100 Hz bandpass Butterworth filter. The data were then segmented in epochs extending from −1000 to +200 ms with respect to button press (*i.e.*, signals were response-locked; the whole analysis has been also performed on stimulus-locked signals, revealing the same statistical effects as obtained with response-locked analysis; for the sake of simplification, we thus focus on the response-locked analysis in the followings). An Independent Component Analysis (ICA) was computed to remove components corresponding to eye blinks, eye movements and electrical line noise (Delorme et al., 2007); signals were screened visually and epochs with residual artifacts were rejected. A current source density (CSD) transformation was subsequently applied to the scalp voltage data. By acting as an efficient source separation method and reducing the skull-induced volume conduction (Vidal et al., 2015), the CSD transformation allowed us to strongly enhance the spatial specificity of the signals (McTeague et al., 2015; Burle et al., 2016), providing a fair estimate of the corticogram (Tenke and Kayser, 2012).

The epochs associated with correct responses were selected and classified according to the trial type (*i.e.*, I-Cue$_{For}$, I-Cue$_{Neutral}$ and I-Cue$_{Against}$ trials). Signals recorded at the C3 and C4 electrode locations were then selected and classified as either contralateral or ipsilateral to the response (Murphy et al., 2016); data were collapsed across response sides. Note that as the analysis focused on correct responses, pooling together left and right responses was equivalent to grouping left and right motion directions. Event-related potential (ERP) and event-related spectral power (ERSP) analyses were subsequently realized for both hemispheres (contralateral, ipsilateral) and each trial type.

In the ERP analysis, the signals were averaged across epochs to attenuate the contribution of neural activity that was not phase-locked to the onset of the button press (Derosiere et al., 2015; Burle et al., 2016). A baseline subtraction was realized on the resulting ERP waveforms. The time window exploited for baseline correction extended from −900 to −600 ms with respect to the button press. This time window was defined based on the RTs of the subjects which ranged between 375 ms and 575 ms across subjects. Hence, stimuli occurred between −575 ms and −375 ms with respect to the response and the period exploited for baseline correction did not overlap with stimulus occurrence or with the resulting visual-evoked potential. Signals were subsequently cropped between −600 and 0 ms in order to focus on the decision-making processes occurring before response execution.

In the ERSP analysis, a time-frequency distribution was calculated for each epoch using a Short-Time Fast-Fourier Transform (ST-FFT; Zhang et al., 2012), with a fixed Hanning window of 250 ms width. The explored frequencies ranged from 1 to 100 Hz in steps of 0.33 Hz (*i.e.*, 300 frequency lines), and the latencies extended from −1000 to +200 ms in steps of 1 ms. On the resulting maps, the value of each time-frequency point was baseline-corrected using a time window ranging from −900 to −600 ms (z-score correction; Hu et al., 2014). As in the ERP analysis, the maps were then cropped between −600 and 0 ms. The baseline correction yielded an ERSP response in which positive and negative spectral power values corresponded to event-related synchronization and desynchronization, respectively (Grandchamp and Delorme, 2011). The epochs were finally averaged together.

Hence, six ERP waveforms and six ERSP maps were obtained in each subject. That is, we obtained a waveform and a map for both hemispheres (contralateral, ipsilateral) and for the three trial types (I-Cue$_{For}$, I-Cue$_{Neutral}$, I-Cue$_{Against}$ trials). Cluster-based statistical analyses were used to assess the effect of the factors HEMISPHERE and TRIAL on these data (Maris and Oostenveld, 2007), as described below.

2.7. Statistical analyses

2.7.1. Behavioral data

Behavioral data were analyzed using Statistica software (version 7.0, Statsoft, Oklahoma, United-States). We performed repeated-measures analyses of variance (ANOVA$_{RM}$) on accuracy and RT data with TRIAL (I-Cue$_{For}$, I-Cue$_{Neutral}$, I-Cue$_{Against}$) as a within-subject factor. When appropriate, Fisher's LSD post-hoc tests were used to detect paired differences. The significance level was set at $p < .05$. Results are expressed as mean ± SE.

2.7.2. EEG data

Cluster-based statistical analyses were used to assess the effect of the factors HEMISPHERE (contralateral, ipsilateral) and TRIAL (I-Cue$_{For}$, I-Cue$_{Neutral}$, I-Cue$_{Against}$) on: *(1)* the potential amplitudes among the multiple time-points composing the ERP waveforms and *(2)* the spectral power among both the time-points and the different frequencies composing the ERSP maps. The cluster-based analyses involved two main steps.

In a first step, an ANOVA was performed for each data point in the ERP and the ERSP analyses using the factors mentioned above. F-values exceeding an alpha level of $p = .05$ were selected and clustered in connected sets based on their temporal adjacency in the ERP analyses and based on both their temporal and frequency adjacencies in the ERSP analyses. Cluster-level F-values were subsequently computed as the sum of each individual F-value.

In a second step, to account for the multiple-comparison problem resulting from the ANOVAs performed in step 1, Monte-Carlo permutation tests were performed. For each subject, data were randomly permuted across conditions, resulting in a so-called "random partition" (separate analyses on ERP signals and ERSP maps). This step can be considered as equivalent to randomly switching the labels of the data, independently for each subject. Based on the random partition, a point-by-point ANOVA was performed in the exact same manner as during step 1. The random partitioning and the subsequent calculation of the cluster-level F-values were re-iterated 1000 times. A histogram of the F-values was then constructed. For each tested effect, the proportion of random partitions that resulted in larger F-values than the observed one was finally calculated. This proportion represents the Monte-Carlo significance probability, also called p-value. If, for a given effect and a given data point, less than 5% of the random partitions resulted in a larger F-value than the one observed in the first step of the analysis, then it is considered as significant for that data point at $p < .05$.

When a significant effect involved more than two conditions, post-hoc tests were required to test which pairwise difference(s) drove the statistical difference detected. For each condition, the values of every data point composing the significant cluster were averaged into a sin-

gle value; Fisher's LSD post-hoc tests were used to detect paired differences on the averaged values.

3. Results

3.1. Behavior

3.1.1. Reaction time

The $ANOVA_{RM}$ performed on the RT data revealed a significant main effect of the factor TRIAL ($F_{2,34} = 7.69$, $p = .001$; Fig. 3A). Specifically, RTs were significantly shorter in $I\text{-}Cue_{For}$ (484 ± 12 ms) than in $I\text{-}Cue_{Neutral}$ (494 ± 13 ms) and $I\text{-}Cue_{Against}$ trials (501 ± 13 ms; $p = .027$ and .0004, respectively). Further, an additional analysis of the RT data including the factor BLOCK did not reveal any significant change in RT over the course of the experiment (main effect of BLOCK: $F_{2,408} = 1.979$, $p = .13$; TRIAL*BLOCK interaction: $F_{7,\ 408} = 0.19$, $p = .99$), indicating that the effect of TRIAL on RTs did not vary over time. Hence, subjects were faster to select the correct action when the implicit color cue provided them with additional evidence regarding that response (*i.e.*, in trials involving a frequent color-motion association). Conversely, they tended to slow down their decision time when the implicit cue yielded evidence against the selection of the correct response (*i.e.*, in trials involving an unlikely color-motion association; $p = .11$ when comparing $I\text{-}Cue_{Against}$ and $I\text{-}Cue_{Neutral}$ trials), in accordance with previous observations (Alamia et al., 2016, 2018).

3.1.2. Accuracy

The $ANOVA_{RM}$ performed on the accuracy data also revealed a significant main effect of the factor TRIAL ($F_{2,34} = 4.15$, $p = .024$; Fig. 3B). As such, accuracy was significantly higher in $I\text{-}Cue_{For}$ trials (0.826 ± 0.012) than in the $I\text{-}Cue_{Against}$ ones (0.788 ± 0.017; $p = .007$); although not significant, subjects also tended to be more accurate in $I\text{-}Cue_{For}$ than in $I\text{-}Cue_{Neutral}$ trials (0.803 ± 0.010; $p = .092$). Accuracy was comparable in $I\text{-}Cue_{Neutral}$ and $I\text{-}Cue_{Against}$ trials ($p = .274$). An additional analysis of the accuracy data including the factor BLOCK did not reveal any significant change in accuracy over the course of the experiment (main effect of BLOCK: $F_{2,408} = 1.848$, $p = .08$; TRIAL*BLOCK interaction: $F_{7,\ 408} = 0.44$, $p = .94$), indicating that the effect of TRIAL on accuracy did not vary over time. Hence, subjects were better at selecting the correct action when the implicit cue provided them with additional information regarding the correct response, as observed in previous studies (Alamia et al., 2016). Conversely, no significant change in decision accuracy was observed in trials where the implicit cue yielded evidence against the selection of the correct response.

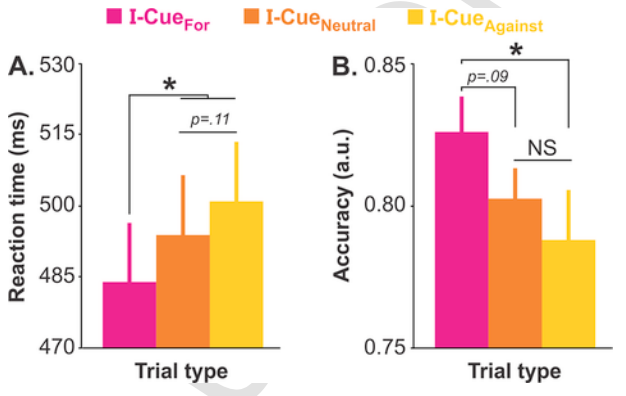

Fig. 3. Impact of the factor TRIAL on the RT (A) and accuracy (B) data. Group-level means ± SEs are represented for the $I\text{-}Cue_{For}$ (pink), $I\text{-}Cue_{Neutral}$ (orange) and $I\text{-}Cue_{Against}$ (yellow) trials. *: Significant difference at $p < .05$. NS: No-Significant. (For interpretation of the references to color in this figure legend, the reader is referred to the Web version of this article.)

3.2. EEG

3.2.1. Event-related potentials (ERPs)

Grand-average ERP waveforms and topographies are provided in Fig. 4. The cluster-based analysis revealed a significant main effect of the factor HEMISPHERE on a cluster of data points, extending from −155 to −40 ms with respect to the motor response (Fig. 4A). As expected for this time window, the amplitude of the ERP was significantly higher (*i.e.*, more negative) in the contralateral than in the ipsilateral hemisphere ($p < .0001$). Besides, no significant effect of the factor TRIAL, nor of its interaction with the factor HEMISPHERE, was found on the ERP data (Fig. 4B and C). Hence, the ERP analysis revealed a buildup of choice-selective activity during the selection process: activity became stronger over the motor cortex contralateral to the chosen finger as movement execution drew nearer. This effect did not depend on whether the implicit cue yielded evidence *for* or *against* its selection.

3.2.2. Event-related spectral power (ERSP)

Grand-average ERSP maps, topographies and post-hoc results are provided in Figs. 5–7. The cluster-based analysis revealed a significant main effect of the factor HEMISPHERE on two clusters of the ERSP data points (Fig. 5A). A first cluster extended from −150 to 0 ms with respect to the motor response and spread from 1 to 7 Hz, corresponding to low frequency oscillations (LFO). In this time-frequency window, the ERSP was significantly higher (*i.e.*, stronger synchronization) in the contralateral than in the ipsilateral hemisphere ($p = .001$; see Fig. 5B to D). A second cluster expanded from −190 to 0 ms and spread from 22 to 27 Hz, corresponding to beta frequency oscillations (BFO). Here, the ERSP was significantly lower (*i.e.*, stronger desynchronization/β-ERD) in the contralateral than in the ipsilateral hemisphere ($p = .033$, Fig. 5B to D, left). Hence, similarly to the ERPs, the spectral power also revealed a buildup of choice-selective activity during the selection process: the contralateral motor cortex exhibited a more pronounced synchronization of LFO and a stronger desynchronization of BFO as movement execution approached compared to the ipsilateral one.

Interestingly, our cluster-based analysis also revealed a significant main effect of the factor TRIAL on two clusters of data points centered on the LFO and the BFO (Fig. 6A, *centre*). A first cluster extended from −290 to 0 ms with respect to the response and spread from 1 to 7 Hz (LFO). In this window, LFO were more synchronized in $I\text{-}Cue_{For}$ than in $I\text{-}Cue_{Against}$ trials ($p = .001$). Further, LFO synchronization tended to be stronger in $I\text{-}Cue_{For}$ trials, and weaker in $I\text{-}Cue_{Against}$ trials, compared to $I\text{-}Cue_{Neutral}$ ones ($p = .097$ and .067, respectively; see Fig. 6B and C). A second cluster expanded from −350 to 0 ms and spread from 14 to 35 Hz, encompassing thus the whole range of BFO. Here, BFO showed a stronger desynchronization (*i.e.*, stronger β-ERD) in $I\text{-}Cue_{For}$ trials than in $I\text{-}Cue_{Against}$ ones ($p < .0001$; comparison with $I\text{-}Cue_{Neutral}$ trials: $p = .112$). Further, BFO was also less desynchronized in $I\text{-}Cue_{Against}$ trials than in $I\text{-}Cue_{Neutral}$ ones ($p < .0001$; Fig. 6B and C). Hence, implicit cues induced a bilateral, choice-independent, effect on oscillatory motor activity. Indeed, both motor cortices (*i.e.*, contralateral and ipsilateral to the chosen finger) displayed a more pronounced LFO synchronization and a stronger BFO desynchronization in trials where the implicit cue provided subjects with additional information regarding the correct action to select, compared to when it provided evidence against the correct response.

Most importantly, the HEMISPHERE and TRIAL effects reported above on the BFO interacted together. Indeed, a significant HEMISPHERE*TRIAL interaction was found on a cluster of data points extending from −160 to 0 ms and spreading from 16 to 25 Hz (*i.e.*, corresponding to low BFO), thus overlapping in part (but not entirely) with the data points showing the HEMISPHERE and TRIAL effects (Fig. 7A).

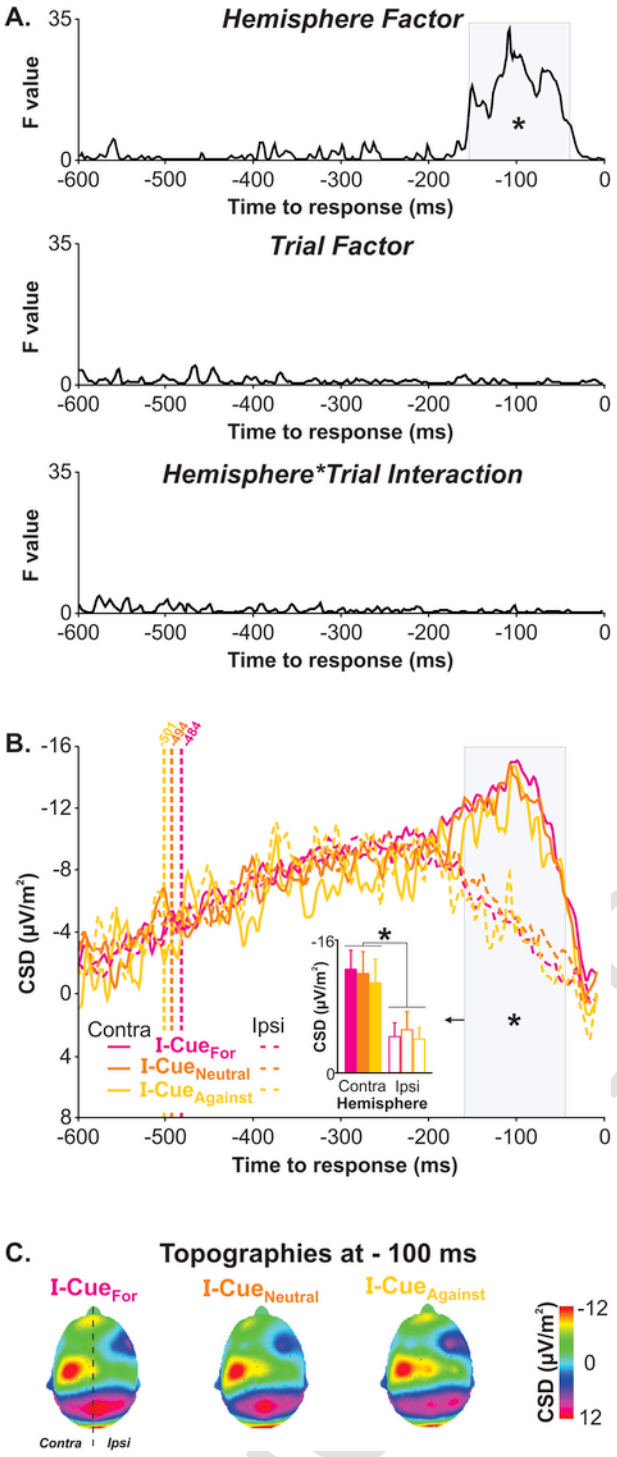

Fig. 4. Impact of the factor HEMISPHERE on the ERP data. A. The cluster-based statistical analysis revealed a significant main effect of the factor HEMISPHERE on a cluster of data points, highlighted by the gray rectangle. **B.** Grand-average ERP waveforms as obtained for the contralateral (solid lines) and ipsilateral (dashed lines) in the I-Cue$_{For}$ (pink), I-Cue$_{Neutral}$ (orange) and I-Cue$_{Against}$ (yellow) trials. The gray rectangle highlights the time window of statistical significance. The small bar graph represents the cluster-level average value (group-level mean ± SE). Vertical lines represent the timing of stimulus occurrence in each trial type (*i.e.*, calculated based on the group-level mean RT). *: Significant difference at $p < .05$. **C.** Grand-average topographies at −100 ms. (For interpretation of the references to color in this figure legend, the reader is referred to the Web version of this article.)

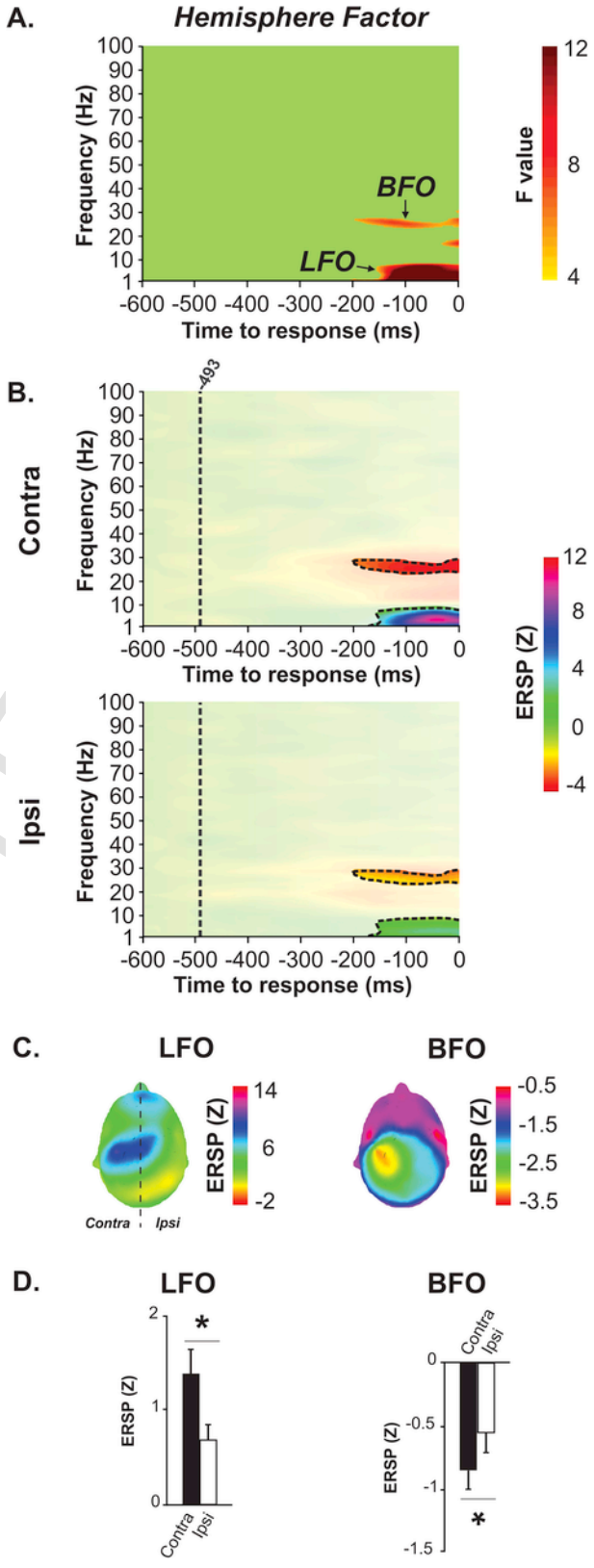

Fig. 5. Impact of the factor HEMISPHERE on the ERSP maps. A. The cluster-based statistical analysis revealed a significant main effect of the factor HEMISPHERE on two clusters of data points (highlighted in orange), centered on the low frequency oscillations and beta frequency oscillations (LFO and BFO, respectively). **B.** Grand-average time-frequency maps as obtained for the contralateral and ipsilateral hemispheres (*top and bottom maps,* respectively; I-Cue$_{For}$, I-Cue$_{Neutral}$ and I-Cue$_{Against}$ trials pooled together). Positive

and negative values represent event-related synchronization and desynchronization, respectively. The time-frequency windows showing a significant HEMISPHERE effect are delineated by black dashed lines. Vertical lines represent the timing of stimulus occurrence (*i.e.*, calculated based on the group-level mean RT; I-Cue$_{For}$, I-Cue$_{Neutral}$ and I-Cue$_{Against}$ trials pooled together). **C.** Grand-average topographies as obtained for the LFO and BFO (obtained at −50 ms/5 Hz and at −120 ms/25 Hz, respectively; I-Cue$_{For}$, I-Cue$_{Neutral}$ and I-Cue$_{Against}$ trials pooled together). **D.** Post-hoc results. Time-frequency boundaries used to calculate the cluster-level average values in each subject are: [-150 to 0 ms]/[1–7 Hz] and [-190 to 0 ms]/[22–27 Hz] (*i.e.*, for the LFO and BFO respectively). Bar graphs represent group-level mean ± SE (I-Cue$_{For}$, I-Cue$_{Neutral}$ and I-Cue$_{Against}$ trials pooled together). *: Significant difference at $p < .05$. (For interpretation of the references to color in this figure legend, the reader is referred to the Web version of this article.)

Hence, the bilateral effect of the factor TRIAL reported above on BFO desynchronization was specific to the high BFO range (25–35 Hz).

In the low BFO range, the type of TRIAL did not significantly alter desynchronization in the ipsilateral hemisphere (I-Cue$_{For}$ vs I-Cue$_{Neutral}$ trials: $p = .759$; I-Cue$_{For}$ vs I-Cue$_{Against}$ trials: $p = .640$; I-Cue$_{Neutral}$ vs I-Cue$_{Against}$ trials: $p = .441$; Fig. 7E), but did so exclusively in the contralateral one. In the latter hemisphere, desynchronization was significantly stronger in I-Cue$_{For}$ trials than in both I-Cue$_{Neutral}$ and I-Cue$_{Against}$ ones ($p = .002$ and < 0.0001, respectively), while it was weaker in I-Cue$_{Against}$ trials than in I-Cue$_{Neutral}$ ones ($p = .042$). Consequently, desynchronization was stronger in the contralateral than in the ipsilateral hemisphere in both I-Cue$_{For}$ and I-Cue$_{Neutral}$ trials ($p = .001$ and $= 0.016$), while it was comparable in the two hemispheres in I-Cue$_{Against}$ trials ($p = .439$). Hence, implicit cues altered low BFO desynchronization in a choice-selective way. Desynchronization was increased (reduced) in trials where the implicit cue provided subjects with evidence for (against) the selection of the correct response specifically in the motor cortex contralateral to the chosen finger.

3.3. Relationship between the behavioral data and low BFO desynchronization

Our results indicate a significant effect of the implicit cues on *(1)* decision speed and accuracy (Fig. 3) and on *(2)* low BFO desynchronization in the contralateral hemisphere (Fig. 7). As a second-level analysis, we assessed the relationship between these two effects.

To do so, we exploited the data measured in I-Cue$_{For}$ and I-Cue$_{Against}$ trials. For each subject, both hemispheres and both trial types, the values of the data points composing the low BFO cluster that showed the significant HEMISPHERE*TRIAL interaction were first averaged together. The cluster-level values obtained for the ipsilateral hemisphere were subsequently subtracted from the values computed for the contralateral one. This subtraction provided us with an indicator of low BFO lateralization (BFO-Lat; Deiber et al., 2012); the lower the BFO-Lat, the stronger the desynchronization in the contralateral hemisphere relative to the ipsilateral one (*i.e.*, the stronger the lateralization). Then, an implicit index was computed for each variable (*i.e.*, for RT,

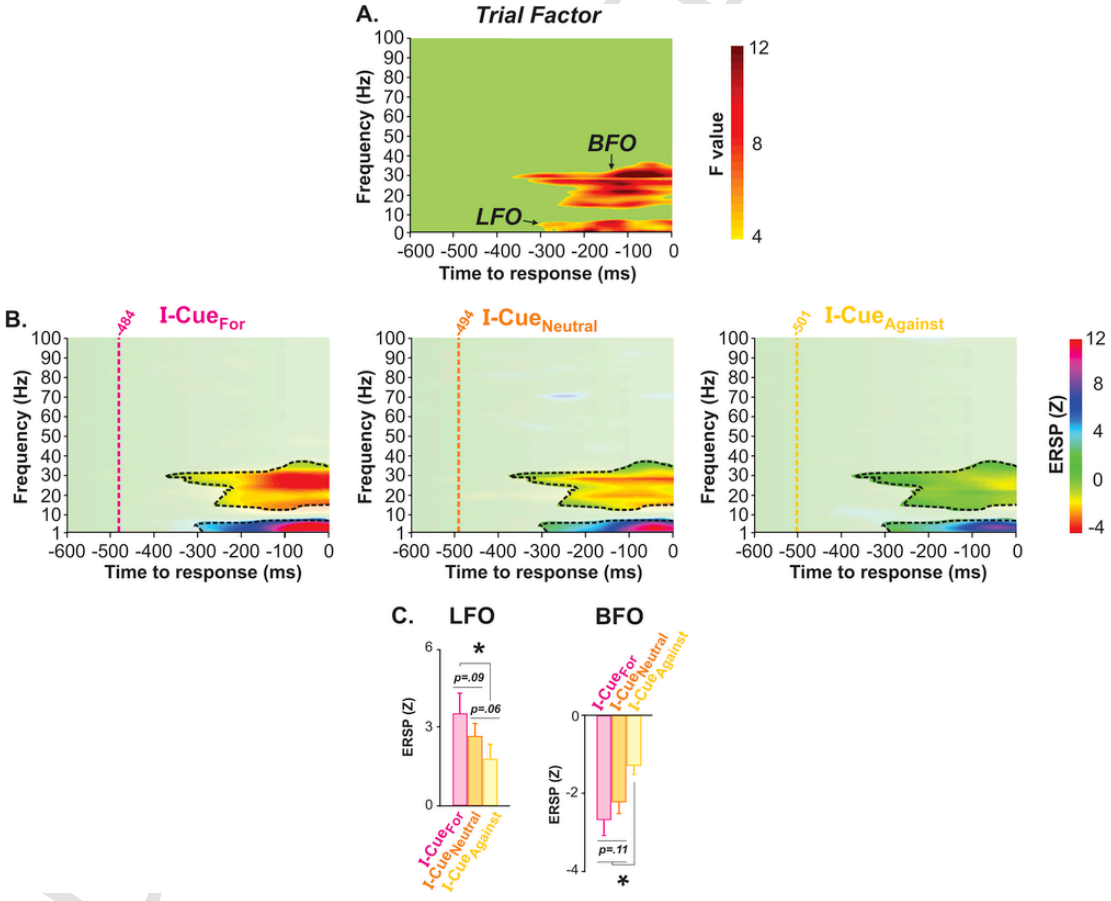

Fig. 6. Impact of the factor TRIAL on the ERSP maps. A. The cluster-based statistical analysis revealed a significant main effect of the factor TRIAL on two clusters of data points (highlighted in orange), centered on the low frequency oscillations and beta frequency oscillations (LFO and BFO, respectively). **B.** Grand-average time-frequency maps as obtained in the I-Cue$_{For}$ (*left map*), I-Cue$_{Neutral}$ (*central map*) and I-Cue$_{Against}$ (*right map*) trials (contralateral and ipsilateral hemispheres pooled together). Positive and negative values represent event-related synchronization and desynchronization, respectively. The time-frequency windows showing a significant TRIAL effect are delineated by black dashed lines. Vertical lines represent the timing of stimulus occurrence in each trial type (*i.e.*, calculated based on the group-level mean RT). Note that red colors depict positive and negative values (*i.e.*, synchronization and desynchronization) for LFOs and BFOs, respectively. **C.** Post-hoc results. Time-frequency boundaries used to calculate the cluster-level average values in each subject are: [-290 to 0 ms]/[1–7 Hz] and [-350 to 0 ms]/[14–35 Hz] (*i.e.*, for the LFO and BFO, respectively). Bar graphs represent group-level mean ± SE (contralateral and ipsilateral hemispheres pooled together). *: Significant difference at $p < .05$. (For interpretation of the references to color in this figure legend, the reader is referred to the Web version of this article.)

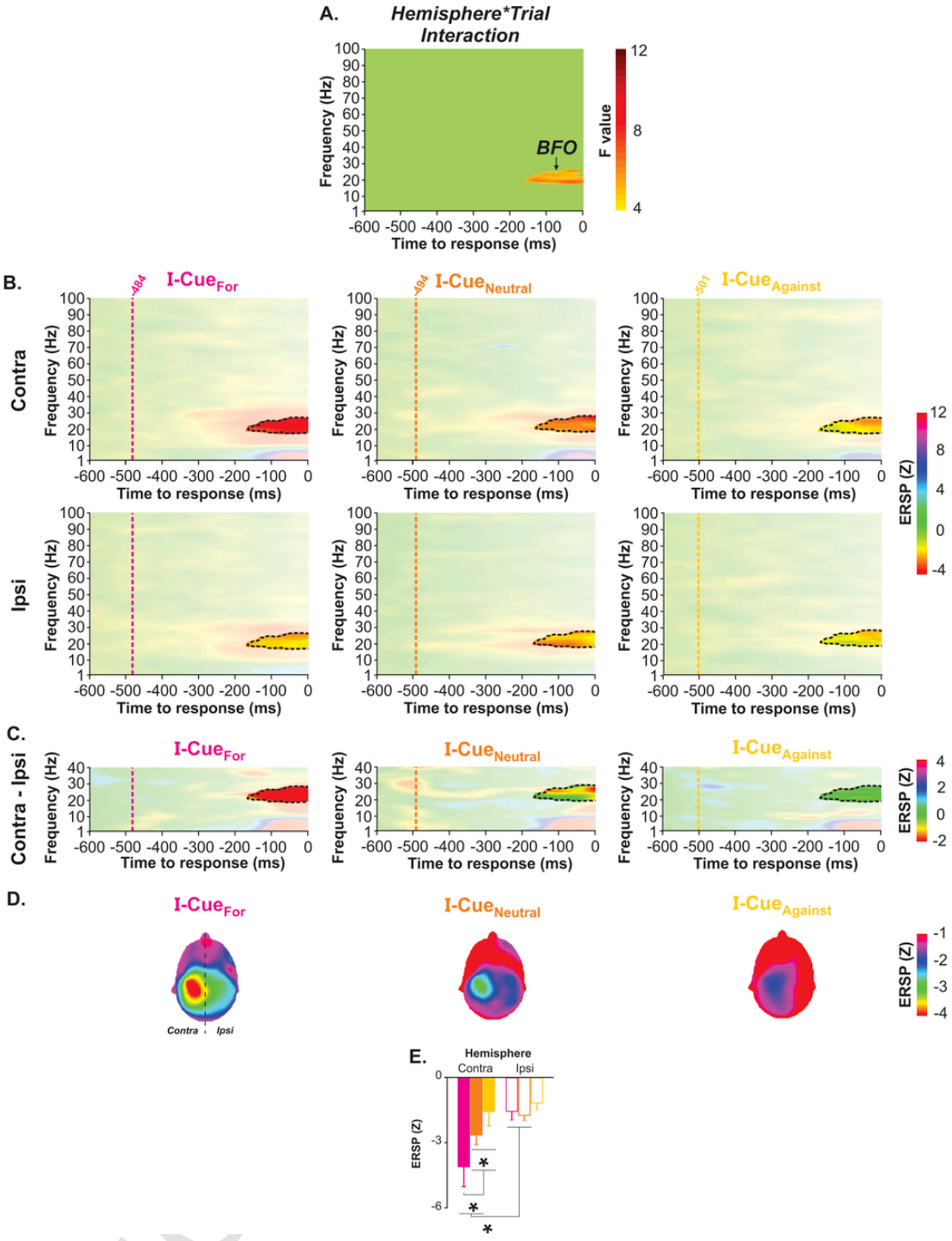

Fig. 7. Impact of the factors HEMISPHERE and TRIAL on the ERSP maps. A. The cluster-based statistical analysis revealed a significant HEMISPHERE*TRIAL interaction on a cluster of data points (highlighted in orange), centered on the low beta frequency oscillations (BFO). **B.** Grand-average time-frequency maps as obtained for the contralateral and ipsilateral hemispheres (*top and bottom rows*, respectively) in the I-Cue$_{For}$ (*left column*), I-Cue$_{Neutral}$ (*central column*) and I-Cue$_{Against}$ (*right column*) trials. Positive and negative values represent event-related synchronization and desynchronization, respectively. The time-frequency window showing a significant HEMISPHERE*TRIAL interaction is delineated by the black dashed lines. **C.** Difference maps obtained from subtracting the values of the data points obtained for the ipsilateral hemisphere from those of the corresponding data points for the contralateral one. The obtained values inform us about the lateralization of the ERSP in I-Cue$_{For}$ (*left column*), I-Cue$_{Neutral}$ (*central column*) and I-Cue$_{Against}$ (*right column*) trials. The time-frequency window showing a significant HEMISPHERE*TRIAL interaction is delineated by black dashed lines. Vertical lines represent the timing of stimulus occurrence in each trial type (*i.e.*, calculated based on the group-level mean RT). **D.** Grand-average topographies as obtained for the LFO and BFO (*top and bottom rows,* respectively). The time-frequency parameters exploited to compute the topographies are provided in brackets. **E.** Post-hoc results. Time-frequency boundaries used to calculate the cluster-level average values in each subject are: [-160 to 0 ms]/[16–25 Hz]. Bar graphs represent group-level mean ± SE. *: Significant difference at $p < .05$. (For interpretation of the references to color in this figure legend, the reader is referred to the Web version of this article.)

accuracy and BFO-Lat) by subtracting the values obtained in I-Cue$_{Against}$ trials from those associated with I-Cue$_{For}$ trials; the larger this index, the stronger the effect of the implicit cue on the considered variable. Spearman correlation analyses were performed to test for any relationship between *(1)* the BFO-Lat and the RT implicit indices and *(2)* the BFO-Lat and the accuracy implicit indices.

Interestingly, the analysis revealed a significant positive correlation between the BFO-Lat and the RT indices (R = 0.63, p = .004; Fig. 8). That is, the more the lateralization of BFO desynchronization increased in I-Cue$_{For}$ trials compared to I-Cue$_{Against}$ ones, the more the RT decreased (*i.e.*, the faster the subjects were to respond) in the former trial type compared to the later one. Importantly, an additional analysis also revealed a positive correlation when the actual BFO desynchronization values obtained in the contralateral hemisphere were exploited to compute the implicit index (*i.e.*, instead of the BFO-Lat values; R = 0.59, p = .011); this correlation was absent when the BFO desynchronization values obtained in the ipsilateral hemisphere were used to compute the implicit index (R = 0.25, p = .319). Therefore, the significant correlation reported between the BFO-Lat and the RT indices was strongly driven by the effect present in the contralateral hemisphere. Besides, the correlation analysis did not reveal a significant link between the BFO-Lat and accuracy indices (R = 0.16, p = .501). Hence, these results suggests that the higher contralateral low BFO desynchronization observed in I-Cue$_{For}$ may have boosted the speed at which the correct response was selected. Conversely, the change in low BFO desynchronization in I-Cue$_{For}$ trials does not seem to account for the higher accuracy of subjects in this condition.

4. Discussion

This study examined the impact of implicit visual cues on motor cortical activity during decision-making. EEG was recorded while participants had to select between left and right index responses according to the motion direction of a cloud of dots which was presented in one of three colors. Unbeknown to the participants, two colors were frequently associated with a given direction, providing them with evidence for the selection of the correct response (I-Cue$_{For}$ trials). When presented with the opposite direction, these two colors yielded evidence against the selection of the correct response (I-Cue$_{Against}$ trials). The third color appeared in equal proportions for both directions and was uninformative (I-Cue$_{Neutral}$ trials). As expected, subjects required a shorter (longer) amount of time, and showed a higher (lower) propensity, to select the correct response in I-Cue$_{For}$ (I-Cue$_{Against}$) trials compared to I-Cue$_{Neutral}$ ones. Interestingly, LFO synchronization (1–7 Hz) and high BFO desynchronization (25–35 Hz) were stronger in I-Cue$_{For}$ than in I-Cue$_{Against}$ trials, in both motor cortices (*i.e.*, contralateral or ipsilateral to the chosen finger), indicating a bilateral impact of the implicit cues on neural activity. Further, implicit cues altered low BFO desynchronization (16–25 Hz) in a choice-selective way. Indeed, low BFO desynchronization was increased in I-Cue$_{For}$ and reduced in I-Cue$_{Against}$ trials (compared to I-Cue$_{Neutral}$ ones) in the motor cortex contralateral to the chosen finger, while it was comparable across trial types in the ipsilateral one. The relevance of the latter effect for behavior was substantiated by a positive correlation, showing that individuals who presented the strongest impact of the implicit cues on low BFO desynchronization were also those whose decision speed was the most boosted by the cues.

4.1. The informative value of the color cues remained implicit

One chief issue in the current study regards to whether subjects remained unconscious about the informative value of the color cues. Our data indicate that it was the case. Indeed, all participants answered negatively to the questionnaire provided at the end of the experiment, and previous studies with an identical experimental design showed that negative answers to questionnaires are associated with failures to report associations in the so-called generative and familiarity tests, classically used to evaluate participants' awareness of an experimental manipulation (Destrebecqz and Peigneux, 2005; Alamia et al., 2016). Furthermore, it is sensible to assume that any subject aware of the informative value of the color would have based her/his choices mostly on it, as detecting the color is easier than discriminating the dominant motion direction of the cloud of dots (the latter being "noisy"). Such a shift from motion-to color-based decisions would have produced drastic between-condition differences – *i.e.*, a substantial boost in decision speed and accuracy would have been then observed in I-Cue$_{For}$ trials. Yet, we did not observe such large effects in our dataset. Instead, the color cue only altered decision speed and accuracy to a small extent with no significant evolution over the course of the experiment, compatible with effects reported in similar studies on implicit processing (Alamia et al., 2016; Derosiere et al., 2017a, 2017b). Altogether, these results indicate that subjects were unaware of the informative value of the color cues.

4.2. Motor cortex exhibited choice-selective activity

Decision-making was associated with a prominent activity in the motor cortex contralateral to the chosen index finger. Indeed, ERP amplitude, LFO synchronization (1–7 Hz) and BFO desynchronization (22–27 Hz) all became larger in the contralateral than in the ipsilateral motor cortex from approximately −200 ms preceding movement onset. These findings corroborate previous observations from the literature in-

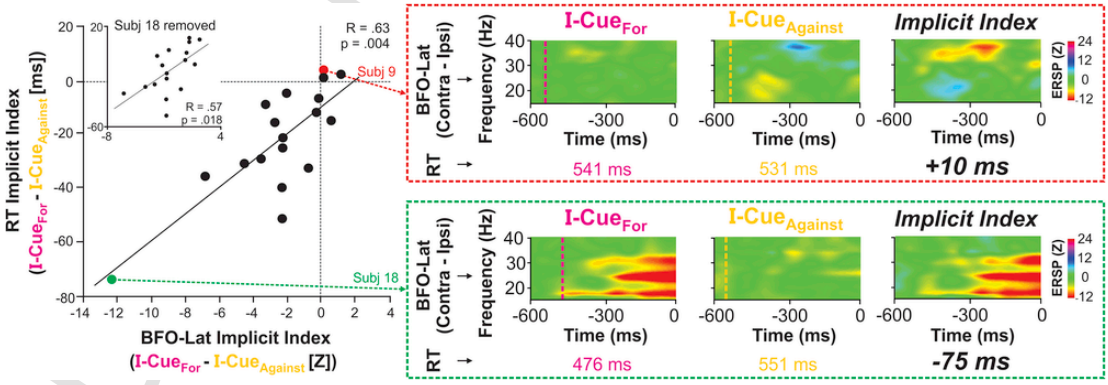

Fig. 8. Relationship between the impact of the implicit cues on the lateralization of BFO desynchronization (BFO-Lat; x-axis) and on RTs (y-axis). The correlation presented in the left panel was performed on implicit indices computed as the difference between the values obtained in I-Cue$_{For}$ trials and those obtained in I-Cue$_{Against}$ trials (see main text). The small inset depicts the correlation when subject 18 (*i.e.*, presenting extreme values) is removed. Right panel shows the BFO-Lat maps (*i.e.*, computed as [contralateral map – ipsilateral map]) and the RT values of two subjects. Vertical lines represent the timing of stimulus occurrence in I-Cue$_{For}$ (pink) and I-Cue$_{Against}$ (yellow) trials for each subject. Subject 9 (red rectangle) did not show any apparent increase in BFO-Lat in I-Cue$_{For}$ compared to I-Cue$_{Against}$ trials. Similarly, this subject's RT was comparable in the former and the latter trial type (+10 ms). Conversely, subject 18 displayed a relative increase in BFO-Lat in I-Cue$_{For}$ compared to I-Cue$_{Against}$ trials and exhibited a strong reduction in RT in the former trial type compared to the latter one (−75 ms). (For interpretation of the references to color in this figure legend, the reader is referred to the Web version of this article.)

dicating that the motor cortex displays a buildup of choice-selective activity during decision-making (Nguyen et al., 2014; Noorbaloochi et al., 2015; Murphy et al., 2016). Our main goal was to examine the impact of implicit visual cues on these decision-related changes in motor activity.

4.3. Implicit cues tuned oscillatory motor activity in a choice-independent way

A key, yet unexpected, finding is that implicit cues induced a bilateral, choice-independent modulation of oscillatory activity, occurring in both the contralateral and ipsilateral motor cortex. LFO synchronization and high BFO desynchronization were indeed stronger when the implicit cue provided evidence for the selection of the correct action, compared to when it provided evidence against the correct response, independently of the considered motor cortex. What may explain such a bilateral modulation of motor activity with implicit cues? One possibility is that it has to do with the level of certainty regarding the appropriate action to select. Indeed, previous work has shown that increasing certainty about which action to select (*i.e.*, as in I-Cue$_{For}$ trials) leads to an overall increase in neural activity in the motor system (Bestmann et al., 2008; Gould et al., 2012; Cirillo et al., 2018). This global boost is thought to bring activity closer to the decision threshold, reducing the impact of new evidence bearing on the decision (de Lange et al., 2010, 2011; Gould et al., 2012). Conversely, when certainty is reduced due to the presence of sensory conflict (*i.e.*, as in I-Cue$_{Against}$ trials), the motor system exhibits a global lowering of activity (Wessel and Aron, 2017), consistent with the presence of a "hold your horse" signal (Frank, 2006). Here, a global reduction of motor activity might increase the distance-to-threshold, allowing time for more evidence to accumulate to do the "right thing". Hence, implicit visual cues may tune motor activity in a nonselective way to bring it either closer or further away from the decision threshold depending on response certainty.

4.4. Implicit cues tuned oscillatory motor activity in a choice-selective way

Interestingly, the impact of implicit cues on part of BFO desynchronization (*i.e.*, in the low BFO range [16–25 Hz]) was specific to the contralateral motor cortex. In fact, low BFO desynchronization in the contralateral motor cortex was stronger (weaker) when the implicit cue provided evidence for (against) the selection of the correct response compared to when it was uninformative, while desynchronization was comparable across trial types in the ipsilateral motor cortex. Hence, in addition to the bilateral tuning of motor activity described above, implicit cues also altered motor activity in a choice-selective way. This effect is reminiscent of the findings of former studies showing that the buildup rate of choice-selective motor activity scales with the strength of evidence present in the visual world (Donner et al., 2009; Gould et al., 2012; Wyart et al., 2012; Tosoni et al., 2014). Importantly though, most previous work has focused on the impact of sensory evidence that was provided explicitly and thus processed consciously. The current findings therefore yield a critical extension of prior observations by indicating that choice-selective activity in motor regions reflects the integration of both explicit and implicit sources of evidence. Such an integration may occur in the visual cortex (*i.e.*, in the case of visual stimuli), which may provide a weighted estimate of the amount of evidence in favor of each action choice to the motor system (de Lange et al., 2013).

4.5. The impact of implicit cues on low BFOs predicted RTs

The extent to which implicit cues altered low BFO desynchronization in a given subject partly predicted the subject's shift in decision speed induced by the cues. Indeed, the more the I-Cue$_{For}$ enhanced low BFO desynchronization in the contralateral motor cortex specifically, the larger the gain was on the response speed. This finding is consistent with the proposal that BFO desynchronization and synchronization are associated with readiness to move and maintenance of stillness, respectively (Tzagarakis et al., 2010). In fact, a similar relationship between BFO desynchronization and RT has been observed in different RT tasks (Misra et al., 2017; van Wijk et al., 2017). Most compellingly, modulation of beta power through motor cortex stimulation was found to alter the speed of motor behaviors (Pogosyan et al., 2009; Joundi et al., 2012), suggesting a causal role of BFO in the generation of speeded movements. The correlation we observed might go a step further with respect to former studies though, as it does not indicate a mere relationship between *absolute* beta power and RT values but instead highlights a link between *relative* values depicting the impact of implicit cues on each variable (*i.e.*, beta power and RT). Hence, given the causal relationship formerly described between beta power and RTs, one may reasonably suggest that the shift in response speed induced by implicit cues was driven by the modulation of choice-selective beta oscillations.

4.6. Implicit cues did not alter motor-related ERPs

Contrary to oscillations, motor-related ERPs were unaffected by implicit cues. An old, yet still accepted, view is that changes in oscillatory activity stem from interconnections occurring between the recorded area and distant brain structures (*i.e.*, through recurrent [sub]cortico-cortical loops), while ERPs emerge as a result of synchronous afferent inputs to the neurons of the recorded area (Pfurtscheller and Lopes, 1999; Engel et al., 2001). Based on the present findings, one may thus assume that integration of implicit information during decision-making entails the recruitment of recurrent loops and does not rely on the mere entry of synaptic inputs to the motor cortex. Such loops may occur between the visual and the motor cortex (*i.e.*, the former continuously providing an estimation of sensory evidence to the latter; Cisek, 2012), and between both motor cortices (*i.e.*, inhibiting each other through mutual inhibition to "win the competition"; Shen et al., 2010). Note though that a previous study revealed an impact of subliminal priming stimuli on motor-related ERPs (Dehaene et al., 1998). Hence, distinct neural mechanisms may be involved in the integration of implicit information depending on whether it is provided through supraliminal (as in the present study) or subliminal stimuli (as in Dehaene et al., 1998), an issue for future investigation.

4.7. Methodological considerations

An alternative explanation of the results observed in the present study would be that the larger synchronization/desynchronization in I-Cue$_{For}$ trials compared to I-Cue$_{Against}$ ones were due to lower/higher baseline activity in the former trial type compared to the latter one. Nonetheless, it is reasonable to assume that the task design did not induce any difference in baseline activity between the three trial types. Indeed, the trial types only differed in terms of the informative value of the implicit color cue, which was only presented to the subjects when the cloud of dots appeared. Hence, subjects were in the exact same experimental conditions in each of the three trial types up to stimulus occurrence and, importantly, the time window exploited for baseline correction corresponded to the pre-stimulus period. Therefore, it is very unlikely that differences in baseline activity altered the relative changes in oscillatory activity measured during decision-making.

One may suggest that the changes in LFOs measured in the present study over central electrodes might reflect an influence of the so-called midfrontal theta (MFT) activity, which covers frequencies ranging between 4 and 8 Hz (Derosiere et al., 2018; Gulbinaite et al., 2014). How-

ever, two major points let us think that it was not the case. First, we found a significantly lower LFO synchronization in trials where the explicit motion information and the implicit color information were in conflict and called for opposite responses (*i.e.*, $I\text{-}Cue_{Against}$ trials) compared to trials in which both information called for the same response (*i.e.*, $I\text{-}Cue_{For}$ trials). Oppositely, MFT activity is well-known to be significantly higher in the face of conflicting trials (Gulbinaite et al., 2014; Töllner et al., 2017; Vissers et al., 2018) or contexts (Derosiere et al., 2018; Van Driel et al., 2015) than in non-conflicting ones. Second, LFO synchronization was lateralized in the present study, with a significantly stronger synchronization over the central electrodes contralateral to the responding hand than over the ipsilateral ones. In contrast, conflict-related MFT activity is usually centered over midline electrodes, with no lateralization with respect to the responding hand reported to date (Derosiere et al., 2018; Gulbinaite et al., 2014; Töllner et al., 2017; Van Driel et al., 2015; Vissers et al., 2018). Hence, the changes in oscillatory activity observed in the present study in the low frequency range (*i.e.*, 1–7 Hz) do not to share the functional and spatial features of MFT activity. Given the choice-selective distribution of LFOs, it is sensible to assume that their synchronization before movement reflected an increased activity of the motor cortex, as previously suggested (Waldert et al., 2015; Popovych et al., 2016).

4.8. Conclusion

In conclusion, our findings indicate that implicit visual cues tune choice-selective oscillatory activity in motor regions during decision-making, boosting (weakening) the buildup of contralateral activity when evidence favors (biases against) the selection of the appropriate action. This modulation of motor activity impacts the speed at which the appropriate action is eventually chosen. In addition to its choice-selective impact, implicit information also alters motor activity in a non-specific way: contralateral and ipsilateral activity are globally shifted towards the decision threshold when implicit information increases certainty about which action to select, while it is downregulated when response certainty is reduced.

Acknowledgements

AA and GD were both supported by the Belgian National Funds for Scientific Research (FNRS). AZ was a Senior Research Associate supported by INNOVIRIS. JD was supported by grants from the "Fonds Spéciaux de Recherche" (FSR) of the Université Catholique de Louvain, the Belgian FNRS.

References

Alamia, A., Orban de Xivry, J.-J., San Anton, E., Olivier, E., Cleeremans, A., Zenon, A., 2016. Unconscious associative learning with conscious cues. Neurosci Conscious 1–10, 2016.

Alamia, A., Solopchuk, O., Zénon, A., 2018. Strong conscious cues suppress preferential gaze allocation to unconscious cues. Front. Hum. Neurosci. 12, 1–9.

Bestmann, S., Harrison, L.M., Blankenburg, F., Mars, R.B., Haggard, P., Friston, K.J., Rothwell, J.C., 2008. Influence of uncertainty and surprise on human corticospinal excitability during preparation for action. Curr. Biol. 18, 775–780.

Brainard, D.H., 1997. The Psychophysics toolbox. Spatial Vis. 10, 433–436.

Burle, B., van den Wildenberg, W.P.M., Spieser, L., Ridderinkhof, K.R., 2016. Preventing (impulsive) errors: electrophysiological evidence for online inhibitory control over incorrect responses. Psychophysiology 53, 1008–1019.

Cirillo, J., Cowie, M.J., MacDonald, H.J., Byblow, W.D., 2018. Response inhibition activates distinct motor cortical inhibitory processes. J. Neurophysiol. 119, 877–886, Available at: http://www.physiology.org/doi/10.1152/jn.00784.2017.

Cisek, P., Pastor-Bernier, A., 2014. On the challenges and mechanisms of embodied decisions. Philos Trans R Soc B Biol Sci 369, 20130479–20130479 Available at: http://rstb.royalsocietypublishing.org/cgi/doi/10.1098/rstb.2013.0479.

de Lange, F.P., Jensen, O., Dehaene, S., 2010. Accumulation of evidence during sequential decision making: the importance of top-down factors. J. Neurosci. 30, 731–738, Available at: http://www.jneurosci.org/cgi/doi/10.1523/JNEUROSCI.4080-09.2010.

de Lange, F.P., Rahnev, D.A., Donner, T.H., Lau, H., 2013. Prestimulus oscillatory activity over motor cortex reflects perceptual expectations. J. Neurosci. 33, 1400–1410, Available at: http://www.jneurosci.org/cgi/doi/10.1523/JNEUROSCI.1094-12.2013.

de Lange, F.P., van Gaal, S., Lamme, V.A.F., Dehaene, S., 2011. How awareness changes the relative weights of evidence during human decision-making. PLoS Biol. 9.

Dehaene, S., Naccache, L., Le Clec'H, G., Koechlin, E., Mueller, M., Dehaene-Lambertz, G., Van De Moortele, P.F., Le Bihan, D., 1998. Imaging unconscious semantic priming. Nature 395, 597–600.

Deiber, M.-P., Sallard, E., Ludwig, C., Ghezzi, C., Barral, J., Ibañez, V., 2012. EEG alpha activity reflects motor preparation rather than the mode of action selection. Front. Integr. Neurosci. 6, Available at: http://journal.frontiersin.org/article/10.3389/fnint.2012.00059/abstract.

Delorme, A., Sejnowski, T., Makeig, S., 2007. Enhanced detection of artifacts in EEG data using higher-order statistics and independent component analysis. Neuroimage 34, 1443–1449.

Derosiere, G., Vassiliadis, P., Demaret, S., Zénon, A., Duque, J., 2017a. Learning stage-dependent effect of M1 disruption on value-based motor decisions. Neuroimage 162, 173–185.

Derosiere, G., Zénon, A., Alamia, A., Duque, J., 2017b. Primary motor cortex contributes to the implementation of implicit value-based rules during motor decisions. Neuroimage 146, 1115–1127.

Destrebecqz, A., Peigneux, P., 2005. Methods for studying unconscious learning. Prog. Brain Res. 150, 69–80.

Donner, T.H., Siegel, M., Fries, P., Engel, A.K., 2009. Buildup of choice-predictive activity in human motor cortex during perceptual decision making. Curr. Biol. 19, 1581–1585.

Engel, A.K., Fries, P., Singer, W., 2001. Dynamic predictions: oscillations and synchrony in top–down processing. Nat. Rev. Neurosci. 2, 704–716.

Frank, M.J., 2006. Hold your horses: a dynamic computational role for the subthalamic nucleus in decision making. Neural Network. 19, 1120–1136.

Gaillard, V., Cleeremans, A., Destrebecqz, A., 2014. Dissociating conscious and unconscious learning with objective and subjective measures. Clin. EEG Neurosci. 45, 50–56.

Gould, I.C., Nobre, A.C., Wyart, V., Rushworth, M.F.S., 2012. Effects of decision variables and intraparietal stimulation on sensorimotor oscillatory activity in the human brain. J. Neurosci. 32, 13805–13818, Available at: http://www.jneurosci.org/cgi/doi/10.1523/JNEUROSCI.2200-12.2012.

Grandchamp, R., Delorme, A., 2011. Single-trial normalization for event-related spectral decomposition reduces sensitivity to noisy trials. Front. Psychol. 2.

Grent-'t-Jong, T., Oostenveld, R., Jensen, O., Medendorp, W.P., Praamstra, P., 2013. Oscillatory dynamics of response competition in human sensorimotor cortex. Neuroimage 83, 27–34.

Herding, J., Spitzer, B., Blankenburg, F., 2016. Upper beta band oscillations in human premotor cortex encode subjective choices in a vibrotactile comparison task. J. Cognit. Neurosci. 28, 668–679.

Herz, D.M., et al., 2017. Distinct mechanisms mediate speed-accuracy adjustments in cortico-subthalamic networks. Elife 6, 357–381, Available at: http://www.ncbi.nlm.nih.gov/pubmed/28137358%0Ahttp://www.pubmedcentral.nih.gov/articlerender.fcgi?artid=PMC5287713%0Ahttp://elifesciences.org/lookup/doi/10.7554/eLife.21481.

Hu, L., Xiao, P., Zhang, Z.G., Mouraux, A., Iannetti, G.D., 2014. Single-trial time-frequency analysis of electrocortical signals: baseline correction and beyond. Neuroimage 84, 876–887.

Jha, A., Diehl, B., Scott, C., McEvoy, A.W., Nachev, P., 2016. Reversed procrastination by focal disruption of medial frontal cortex. Curr. Biol. 26, 2893–2898.

Joundi, R.A., Brittain, J.S., Green, A.L., Aziz, T.Z., Brown, P., Jenkinson, N., 2012. Oscillatory activity in the subthalamic nucleus during arm reaching in Parkinson's disease. Exp. Neurol. 236, 319–326.

Kubanek, J., Snyder, L.H., Brunton, B.W., Brody, C.D., Schalk, G., 2013. A low-frequency oscillatory neural signal in humans encodes a developing decision variable. Neuroimage 83, 795–808.

Lo, C.C., Wang, X.J., 2006. Cortico-basal ganglia circuit mechanism for a decision threshold in reaction time tasks. Nat. Neurosci. 9, 956–963.

Loughnane, G.M., Newman, D.P., Bellgrove, M.A., Lalor, E.C., Kelly, S.P., O'Connell, R.G., 2016. Target selection signals influence perceptual decisions by modulating the onset and rate of evidence accumulation. Curr. Biol. 26, 496–502.

Maris, E., Oostenveld, R., 2007. Nonparametric statistical testing of EEG- and MEG-data. J. Neurosci. Methods 164, 177–190.

Mayr, U., 2004. Conflict, consciousness, and control. Trends Cognit. Sci. 8, 145–148.

McTeague, L.M., Gruss, L.F., Keil, A., 2015. Aversive learning shapes neuronal orientation tuning in human visual cortex. Nat. Commun. 6.

Meijer, D., te Woerd, E., Praamstra, P., 2016. Timing of beta oscillatory synchronization and temporal prediction of upcoming stimuli. Neuroimage 138, 233–241.

Misra, G., Ofori, E., Chung, J.W., Coombes, S.A., 2017. Pain-related suppression of beta oscillations facilitates voluntary movement. Cerebr. Cortex 27, 2592–2606.

Mouraux, A., Iannetti, G.D., 2008. Across-trial averaging of event-related EEG responses and beyond. Magn. Reson. Imaging 26, 1041–1054.

Murphy, P.R., Boonstra, E., Nieuwenhuis, S., 2016. Global gain modulation generates time-dependent urgency during perceptual choice in humans. Nat. Commun. 7.

Nguyen, V.T., Breakspear, M., Cunnington, R., 2014. Reciprocal interactions of the SMA and cingulate cortex sustain premovement activity for voluntary actions. J. Neurosci. 34, 16397–16407, Available at: http://www.jneurosci.org/lookup/doi/10.1523/JNEUROSCI.2571-14.2014.

Noorbaloochi, S., Sharon, D., McClelland, J.L., 2015. Payoff information biases a Fast guess process in perceptual decision making under deadline pressure: evidence from behavior, evoked potentials, and quantitative model comparison. J. Neurosci. 35, 10989–11011, Available at: http://www.jneurosci.org/cgi/doi/10.1523/JNEUROSCI.0017-15.2015.

Paz, L., Insabato, A., Zylberberg, A., Deco, G., Sigman, M., 2016. Confidence through consensus: a neural mechanism for uncertainty monitoring. Sci. Rep. 6.

Pezzulo, G., Cisek, P., 2016. Navigating the affordance Landscape: feedback control as a process model of behavior and cognition. Trends Cognit. Sci. 20, 414–424, Available at: https://doi.org/10.1016/j.tics.2016.03.013.

Pfurtscheller, G., Lopes, F.H., 1999. Event-related EEG/MEG synchronization and desynchronization: basic principles. Clin. Neurophysiol. 110, 1842–1857.

Pogosyan, A., Gaynor, L.D., Eusebio, A., Brown, P., 2009. Boosting cortical activity at beta-band frequencies slows movement in humans. Curr. Biol. 19, 1637–1641.

Popovych, S., Rosjat, N., Toth, T.I., Wang, B.A., Liu, L., Abdollahi, R.O., Viswanathan, S., Grefkes, C., Fink, G.R., Daun, S., 2016. Movement-related phase locking in the delta–theta frequency band. Neuroimage 139, 439–449.

Shen, K., Kalwarowsky, S., Clarence, W., Brunamonti, E., Paré, M., 2010. Beneficial effects of the NMDA antagonist ketamine on decision processes in visual search. J. Neurosci. 30, 9947–9953.

Sumner, P., Nachev, P., Morris, P., Peters, A.M., Jackson, S.R., Kennard, C., Husain, M., 2007. Human medial frontal cortex mediates unconscious inhibition of voluntary action. Neuron 54, 697–711.

Thura, D., Cisek, P., 2014. Deliberation and commitment in the premotor and primary motor cortex during dynamic decision making. Neuron 81, 1401–1416.

Thura, D., Cisek, P., 2017. The basal ganglia do not select reach targets but control the urgency of commitment. Neuron 95, 1160–1170.e5.

Tosoni, A., Corbetta, M., Calluso, C., Committeri, G., Pezzulo, G., Romani, G.L., Galati, G., 2014. Decision and action planning signals in human posterior parietal cortex during delayed perceptual choices. Eur. J. Neurosci. 39, 1370–1383.

Tosoni, A., Galati, G., Romani, G.L., Corbetta, M., 2008. Sensory-motor mechanisms in human parietal cortex underlie arbitrary visual decisions. Nat. Neurosci. 11, 1446–1453.

Tzagarakis, C., Ince, N.F., Leuthold, A.C., Pellizzer, G., 2010. Beta-band Activity during motor planning reflects response uncertainty. J. Neurosci. 30, 11270–11277, Available at: http://www.jneurosci.org/cgi/doi/10.1523/JNEUROSCI.6026-09.2010.

van Gaal, S., Ridderinkhof, K.R., Scholte, H.S., Lamme, V.A.F., 2010. Unconscious activation of the prefrontal No-go network. J. Neurosci. 30, 4143–4150, Available at: http://www.jneurosci.org/cgi/doi/10.1523/JNEUROSCI.2992-09.2010.

van Wijk, B.C.M., Neumann, W.J., Schneider, G.H., Sander, T.H., Litvak, V., Kühn, A.A., 2017. Low-beta cortico-pallidal coherence decreases during movement and correlates with overall reaction time. Neuroimage 159, 1–8.

Von Reyn, C.R., Breads, P., Peek, M.Y., Zheng, G.Z., Williamson, W.R., Yee, A.L., Leonardo, A., Card, G.M., 2014. A spike-timing mechanism for action selection. Nat. Neurosci. 17, 962–970.

Waldert, S., Vigneswaran, G., Philipp, R., Lemon, R.N., Kraskov, A., 2015. Modulation of the intracortical LFP during action execution and observation. J. Neurosci. 35, 8451–8461, Available at: http://www.jneurosci.org/cgi/doi/10.1523/JNEUROSCI.5137-14.2015.

Wessel, J.R., Aron, A.R., 2017. On the globality of motor suppression: unexpected events and their influence on behavior and cognition. Neuron 93, 259–280.

Wyart, V., de Gardelle, V., Scholl, J., Summerfield, C., 2012. Rhythmic fluctuations in evidence accumulation during decision making in the human brain. Neuron 76, 847–858.

Zhang, Z.G., Hu, L., Hung, Y.S., Mouraux, A., Iannetti, G.D., 2012. Gamma-band oscillations in the primary somatosensory cortex--A direct and obligatory correlate of subjective pain intensity. J. Neurosci. 32, 7429–7438, Available at: http://www.jneurosci.org/cgi/doi/10.1523/JNEUROSCI.5877-11.2012.